## Original Article

# Regional Differences in the Ghrelin-Growth Hormone Secretagogue Receptor Signalling System in Human Heart Disease

Rebecca Sullivan, BSc,[a] Varinder K. Randhawa, PhD, MD,[b] Tyler Lalonde, PhD,[c] Tina Yu, BSc,[d]
Bob Kiaii, MD,[e] Leonard Luyt, PhD,[c,f] Gerald Wisenberg, MD,[d,g,h] and
Savita Dhanvantari, PhD[a,d,g,i]

[a] Pathology and Laboratory Medicine, Western University, London, Ontario, Canada

[b] Cardiology Division, Toronto General Hospital, University Health Network, and University of Toronto, Ontario, Canada

[c] Chemistry, Western University, London, Ontario, Canada

[d] Medical Biophysics, Western University, London, Ontario, Canada

[e] Cardiac Surgery, Western University, London, Ontario, Canada

[f] Oncology, London Regional Cancer Program, Western University, London, Ontario, Canada

[g] Imaging Program, Lawson Health Research Institute, London, Ontario, Canada

[h] Cardiac Imaging Research, Lawson Health Research Institute, London, Ontario, Canada

[i] Metabolism and Diabetes, Lawson Health Research Institute, London, Ontario, Canada

## ABSTRACT

**Background:** The hormone ghrelin and its receptor, the growth hormone secretagogue receptor (GHSR) are expressed in myocardium. GHSR binding activates signalling pathways coupled to cardiomyocyte survival and contractility. These properties have made the ghrelin-GHSR axis a candidate for a biomarker of cardiac function. The dynamics of ghrelin-GHSR are altered significantly in late stages of heart failure (HF) and cardiomyopathy, when left ventricular (LV) function is

## RÉSUMÉ

**Contexte :** L'hormone ghréline et son récepteur, le récepteur sécrétagogue de l'hormone de croissance (GHSR, de l'anglais *growth hormone secretagogue receptor*), sont exprimés dans le myocarde. La liaison au récepteur GHSR active les voies de signalisation associées à la survie et à la contractilité des cardiomyocytes. Ces propriétés font de l'axe ghréline-récepteur GHSR un bon candidat biomarqueur de la fonction cardiaque. En effet, la dynamique de cet

Ghrelin is a peptide hormone that has well known orexigenic effects on the body. Ghrelin is an endogenous 28 amino acid peptide that is a natural ligand of the growth hormone secretagogue receptor (GHSR) 1a, a 7-transmembrane G-protein coupled receptor. More recently, ghrelin has been studied for its effects and role in cardiac energetics through activation of myocardial GHSR. Specifically within cardiomyocytes, the binding of ghrelin to GHSR activates

downstream signalling pathways that lead to cardioprotective effects, such as maintenance of contractility,[1,2] suppression of inflammation,[3,4] and promotion of growth and survival.[5] Cardiac GHSR activation promotes excitation-contraction coupling, increasing $Ca^{2+}$ flux through the sarcoplasmic reticulum ATPase pump (SERCA2a) and the voltage gated $Ca^{2+}$ channels, which produces a positive inotropic effect and protects against ischemia/reperfusion injury in cardiomyocytes.[2] Ghrelin also regulates inflammation in the heart through the protein kinase B (Akt) pathway, decreasing expression of the proinflammatory markers[6] interleukin 1-β, tumour necrosis factor α, and interleukin 6, and upregulating the tumour necrosis factor α/nuclear factor kappa-light-chain-enhancer of activated B cells (NFκB) pathways.[3] Ghrelin has been shown to protect the heart through the toll like receptor 4 (TLR4) pathway.[4] Apoptosis is decreased upon GHSR activation through extracellular signal-related kinases 1/2 and

Sullivan et al.
Regional Ghrelin-GHSR Signalling in Heart Disease

183

failing. We examined the relationship of GHSR with ghrelin in cardiac tissue from patients with valvular disease with no detectable changes in LV function.

**Methods:** Biopsy samples from the left ventricle and left atrium were obtained from 25 patients with valvular disease (of whom 13 also had coronary artery disease) and preserved LV ejection fraction, and compared to control samples obtained via autopsy. Using quantitative confocal fluorescence microscopy, levels of GHSR were determined using [Dpr$^3$(n-octanoyl),Lys$^{19}$(sulfo-Cy5)]ghrelin(1-19), and immuno-fluorescence determined ghrelin, the heart failure marker natriuretic peptide type-B (BNP), and contractility marker sarcoplasmic reticulum ATPase pump (SERCA2a).

**Results:** A positive correlation between GHSR and ghrelin was apparent in only diseased tissue. Ghrelin and BNP significantly correlated in the left ventricle and strongly colocalized to the same intracellular compartment in diseased and control tissue. GHSR, ghrelin, and BNP all strongly and significantly correlated with SERCA2a in the left ventricle of diseased tissue only.

**Conclusions:** Our results suggest that the dynamics of the myocardial ghrelin-GHSR axis is altered in cardiovascular disease in the absence of measurable changes in heart function, and might accompany a regional shift in endocrine programming.

axe est considérablement altérée aux stades avancés de l'insuffisance cardiaque et de la cardiomyopathie, lorsque la fonction ventriculaire gauche décline. Nous avons donc étudié la relation entre le récepteur GHSR et la ghréline dans le tissu cardiaque de patients présentant une valvulopathie sans changements détectables dans la fonction ventriculaire gauche.

**Méthodologie :** Des échantillons de tissus du ventricule et de l'oreillette gauches ont été prélevés par biopsie chez 25 patients présentant une valvulopathie (dont 13 avaient aussi une coronaropathie) et une fraction d'éjection ventriculaire gauche préservée, puis comparés avec des échantillons témoins prélevés à l'autopsie. Les taux du récepteur GHSR ont été mesurés par microscopie en fluorescence confocale quantitative à l'aide de [Dpr$^3$(n-octanoyl),Lys$^{19}$(sulfo-Cy5)] ghréline(1-19); les taux de ghréline, de peptide natriurétique de type B (BNP, un marqueur de l'insuffisance cardiaque), et de pompe ATPase du réticulum sarcoplasmique (SERCA2a; un marqueur de la contractilité) ont quant à eux été mesurés par immunofluorescence.

**Résultats :** Nous avons noté une corrélation positive entre le récepteur GHSR et la ghréline uniquement dans les tissus lésés. Il existe une corrélation significative entre les taux de ghréline et de BNP dans le ventricule gauche, les deux substances étant fortement localisées dans le même compartiment intracellulaire, tant dans les tissus malades que dans les tissus témoins. Le récepteur GHSR, la ghréline et le BNP sont tous fortement et significativement corrélés avec la SERCA2a SERCA2a dans le tissu ventriculaire gauche malade seulement.

**Conclusions :** Nos résultats semblent indiquer que la dynamique de l'axe ghréline-récepteur GHSR dans le myocarde est altérée en cas de maladie cardiovasculaire même en l'absence de changements mesurables de la fonction cardiaque, et que cette altération pourrait être attribuable à une modification régionale de la programmation endocrinienne.

Akt serine kinases[5,6] and inhibition of caspase-3 and -9.[7] Fibrosis deposition is also minimized in the heart after ghrelin administration.[8,9] Therefore, the ghrelin-GHSR axis within the myocardium plays a critical role in the maintenance of cardiomyocyte function and survival.

The discovery of the myocardial ghrelin-GHSR axis and its role in cardiomyocyte function and health has prompted studies on its dynamics in heart failure (HF) and cardiomyopathy. We and others have shown that myocardial GHSR is elevated in HF.[10,11] Additionally, we showed that the cardiac ghrelin-GHSR axis was abnormally upregulated in end-stage HF compared to endomyocardial biopsies from engrafted hearts,[11] thus suggesting that tissue levels of ghrelin and GHSR could be indicators of the health of transplanted hearts. In contrast, one study has reported decreased GHSR in tissue from patients with dilated cardiomyopathy, which negatively correlated with left ventricular (LV) ejection fraction (LVEF).[12] We[13] and others[14] have shown that tissue GHSR also decreased in mouse models of diabetic cardiomyopathy, suggesting that the dynamics of the myocardial ghrelin-GHSR axis might differ in earlier stages of myocardial decompensation compared with end-stage HF.

Some potential causes of HF include coronary artery disease (an accumulation of cholesterol [plaques] in the vessel walls) or aortic stenosis (progressive restriction of the opening of the aortic valve),[15] and there has been some clinical investigation into correlations with serum ghrelin levels and

the effects of ghrelin administration on heart function in these conditions. In humans with coronary artery disease and with diabetes-associated coronary atherosclerosis, serum levels of ghrelin decreased significantly compared with that in healthy control participants.[16,17] Another study also showed an inverse relationship between serum ghrelin and coronary artery disease detected using angiography that was independent of other cardiovascular risk factors,[16] suggesting that a reduction in ghrelin-GHSR signalling might be correlated with progressively more severe coronary artery disease. Ghrelin administration in rats with aortic stenosis reduced calcification build-up in the myocardium in a dose-dependent manner,[18] and attenuated aortic calcium deposition both *in vivo* and *in vitro*.[19] Therefore, investigating the dynamics of the ghrelin-GHSR axis and signalling within cardiomyocytes might provide further insight into the potential use of ghrelin as a therapy for myocardial dysfunction (HF).

In this study, toward the goal of determining the potential of ghrelin-GHSR as a biomarker of heart disease (HD), we examined their levels in a cohort of patients who underwent elective cardiac valve replacement surgery and compared their expression levels with that in control heart tissues. We also determined the correlation of ghrelin-GHSR with an array of biomarkers including natriuretic peptide type-B (BNP), SERCA2a, and toll-like receptor 4 (TLR4). With these data, we hope to obtain further insight into the distinct molecular signalling patterns associated with the progression of HD.

**Table 1.** Cardiac surgery patient demographic characteristics

| Patient condition | Number of men with condition (n = 16) | Number of women with condition (n = 9) |
| --- | --- | --- |
| Age range, years | 49-84 | 45-77 |
| Mean age, years | 69 | 60 |
| Coronary artery disease | 9 | 2 |
| Moderate-severe aortic stenosis | 14 | 8 |
| Hypertension | 8 | 2 |
| High pulmonary artery pressure | 10 | 7 |
| Diabetes | 2 | 1 |
| LVEF < 45% | 2 | 0 |
| LVEF > 45% | 14 | 9 |

LVEF, left ventricular ejection fraction.

**Table 2.** Patient medications post heart surgery

| Patient medication | Number of men with medication (n = 16) | Number of women with medication (n = 9) |
| --- | --- | --- |
| ACE inhibitor | 1 | 2 |
| Antiarrhythmic | 1 | 2 |
| Angiotensin receptor blocker | 6 | 1 |
| Coumadin | 4 | 2 |
| β-Blocker | 5 | 5 |
| Calcium channel blocker | 2 | 3 |
| Diuretic | 8 | 3 |
| Statin | 11 | 3 |

ACE, angiotensin converting enzyme.

## Methods

### Patient cohort

Tissue samples were harvested from 25 patients who underwent aortic valve replacement surgery for aortic stenosis at the London Health Sciences Centre between 2013 and 2014. Twenty-four of these patients had aortic stenosis and one had mitral valve impairment. Of these 25 patients, 11 concurrently had coronary artery disease and received coronary artery bypass grafts. Sixteen patients were male and nine were female, with an overall average age of 66 years. Twenty-three patients had normal ejection fractions (> 45%) before surgery, and 2 patients had reduced ejection fractions (35%-40%). The protocol for obtaining tissue samples was approved by Western University's Health Sciences Research Ethics Board. Tissue samples, approximately 0.2-0.5 cm in length, were collected from the left atrium (LA) and LV myocardium from each patient. The LA samples were obtained from the posterior LA wall just on the LA side of the interatrial septum (close to the right atrium but technically the left atrium). The LV samples were taken from the posterior LV wall, just below the mitral valve. Patient demographic characteristics, cardiac function (LVEF), and medications are shown in Tables 1 and 2. All patient samples and patient data were kept anonymous and all biomarker analyses were completed before receiving clinical data.

To provide a reference nondiseased control, paraffin-embedded and sectioned samples of cardiac tissue (n = 10) were obtained from the tissue archives of the Department of Pathology, London Health Sciences Centre. These tissue samples had been obtained from the left ventricle of patients who had died from noncardiac causes at the time of postmortem, 24-48 hours after the patient was pronounced dead. Of these 10 patients, 5 were male and 5 were female. The average age of all 10 patients was approximately 59 years. Analysis of these tissues was compared to the analysis derived from the surgery patients for overall marker fluorescence intensity and differences in biomarker relationships.

### Quantitative fluorescence microscopy

Samples were fixed, frozen, and embedded in optimal cutting temperature compound, and subsequently sectioned at 6-7 μm thickness, as previously described.[20,21] Immunohistochemistry using primary and fluorophore-conjugated secondary antibodies was conducted as previously described.[20,21]

In brief, tissue sections were incubated with blocking buffer in 10% serum for 30 minutes at room temperature followed by incubation with primary polyclonal or monoclonal antibodies (Table 3) for 1 hour at room temperature in a humidified chamber. These antibodies were used to identify ghrelin (1:100; Santa Cruz Biotechnology), BNP (1:1000; Abcam), SERCA2a (1:300; Abcam), and TLR4 (1:250; Abcam). Samples were rinsed twice in phosphate buffered solution and incubated for 2 hours at room temperature with secondary antibodies (1:500; Table 3). To detect GHSR, we used the far-red ghrelin peptide analogue, [Dpr$^3$(n-octanoyl),Lys$^{19}$(sulfo-Cy5)]ghrelin(1-19), referred to as Cy5-ghrelin(1-19), as we have previously done to quantify GHSR *in situ*.[21] This analogue binds with high specificity to GHSR in mouse and human cardiac tissue samples.[11,13] After incubation with secondary antibodies, Cy5-ghrelin(1-19) was added to tissue sections for 30 minutes. Sections were washed twice with phosphate buffered saline, incubated for 8 minutes with DAPI nuclear stain (1:1000), and mounted with ProLong Diamond antifade (Life Technologies) to prevent the tissues from photobleaching. N numbers for each biochemical marker were different because of the limited amount of tissue available at the time of staining.

For control cardiac tissue, all sections were deparaffinized with decreasing concentrations of alcohol solutions (95%-70%). Samples were then stained as previously stated for the following biomarkers: ghrelin (1:100; Santa Cruz Biotechnology), BNP (1:1000; Abcam), SERCA2a (1:300; Abcam), and TLR4 (1:250; Abcam), and GHSR (1:100) using Cy5-ghrelin(1-19).

### Background subtraction for fluorescence microscopy imaging

To ensure specificity of the fluorescent signal for GHSR, background subtraction was performed, because GHSR has a diffuse staining pattern. To calculate the background signal, tissue sections were first incubated with 100 μM hexarelin, a GHSR ligand[22] known to competitively displace Cy5-ghrelin(1-19),[21] for 1 hour at room temperature before incubation with 10μM Cy5-ghrelin(1-19) as described previously. Tissues were then stained for DAPI (1:1000), washed, and mounted with ProLong Diamond antifade (Life Technologies) as described previously. For control tissue samples, background fluorescence intensity values were calculated in 5 separate control samples, and the average value of these intensities was subtracted from the total fluorescence intensities of GHSR in each of the 10 original tissue samples. For

Sullivan et al.
Regional Ghrelin-GHSR Signalling in Heart Disease

185

**Table 3.** Antibody table; information on antibodies used

| Antigen | Catalog number | Dilution | Host |
|---------|----------------|----------|------|
| Ghrelin | sc-10359 | 1:100 | Goat |
| BNP | ab19645 | 1:1000 | Rabbit |
| SERCA2a | ab3265 | 1:300 | Rabbit |
| TLR4 | ab22048 | 1:250 | Mouse |
| DAPI | 62247 | 1:1000 | — |
| Alexa Fluor 488 | A11055 | 1:1000 | Donkey anti-goat |
| Alexa Fluor 594 | A21207 | 1:1000 | Donkey anti-rabbit |
| Alexa Fluor 488 | A21206 | 1:1000 | Donkey anti-rabbit |
| Alexa Fluor 594 | A21203 | 1:1000 | Donkey anti-mouse |

BNP, natriuretic peptide type-B; SERCA2a, sarcoplasmic reticulum ATPase pump; TLR4, toll like receptor 4.

diseased tissue samples, background values were calculated from 5 fields of view in 1 slide from each patient, and the average value of this slide was calculated as the background fluorescence. These values were subtracted from the total fluorescence intensities of nonblocked tissue from that patient to obtain a specific Cy5-ghrelin(1-19) signal in the diseased tissue.

## Image acquisition and analysis

High resolution images of the diseased and control tissues were captured with a Nikon A1R Confocal Microscope at magnification 60× using an oil immersion lens. Five random fields of view were acquired for each of 2 tissue sections per patient sample with the exposure time, gain, and high/low look up tables set the same for all tissue sections. Therefore, each patient sample (reported as data points in all graphs) reflects an average of 2 technical replicates.

Images of GHSR, ghrelin, BNP, SERCA2a, and TLR4 were analyzed with FIJI 1.49v, a distribution of ImageJ software (National Institutes of Health). Algorithms built into ImageJ were used to quantify different staining patterns in the tissue. Punctate staining patterns were quantified using the RenyiEntropy algorithm, an entropy-based approach that distinguishes the positive punctate signals within the cells from the background. The integrated density represents the mean intensity of the positive signal above a certain threshold in scaled units divided by the area in pixels. The integrated density threshold was set such that the entropies of distributions above and below the set threshold are maximized. Therefore, this algorithm only captured the high-intensity punctate staining patterns and did not calculate any background staining of these images. A representation of what the algorithm identified as positive vs background is shown in Supplemental Figure S1.

For diffuse staining patterns, the Li algorithm was used to quantify the specific fluorescence signal after background subtraction as described previously. All images for diffuse staining were quantified using the built-in ImageJ Li algorithm with the integrated density (stated previously) determined for each tissue.

## Fibrosis imaging

To assess fibrosis, heart tissue sections were stained with Masson's Trichrome stain by the core Pathology Laboratory at London Health Sciences Centre. Sections of the diseased and control tissue were acquired using bright field microscopy at magnification 10× and 20× with a Zeiss Axioskop

EL-Einsatz microscope and Northern Eclipse software as described previously.[11,13] Images were acquired for the entire tissue section and quantification was performed on the entire tissue.

Fibrosis was analyzed using an online script in the program ImageJ Fiji, which quantified the percentage of fibrotic tissue in each sample by distinguishing fibrotic tissue (blue) from non-fibrotic tissue (red), as previously described.[23] Briefly, this script divides the RBG image into each of its channels, which thresholds the image for positive pixels in either the red or blue channels. All tissue sections were set at the same threshold for the fibrotic and nonfibrotic tissue. The fibrosis was then quantified on the basis of the fibrotic tissue compared with the total area of tissue to determine the average percentage of fibrosis in each of the diseased or control tissue samples.

## Data analysis

Data from biomarkers (GHSR, ghrelin, BNP, SERCA2a, and TLR4) were disaggregated according to cardiac region using a post-hoc analysis. Statistical analyses were performed using GraphPad Prism version 8. Unpaired student $t$-tests were used to compare overall biomarker expression differences between the diseased and control tissue. Within the diseased tissue cohort, a 1-way analysis of variance using Tukey post-hoc test to determine regional differences. Linear regression was used to determine correlations between the following biomarkers: GHSR, ghrelin, BNP, SERCA2a, and TLR4. Linear regression analysis was used to compare biomarker fluorescence intensities on the basis of the following categories: entire patient cohort and regional differences (left atrium and left ventricle). Pearson correlation was used to determine colocalization between ghrelin and BNP in diseased (LA and LV) and control tissue. All statistical analyses were completed with significance set at $P < 0.05$.

## Results

### Cardiac surgery patient cohort

Of the 25 patients who underwent cardiac surgery, 16 were male and 9 were female with mean ages of 69 and 60, respectively (Table 1). The patients had a range of moderate to severe aortic stenosis whereas 11 also had coronary artery disease. In the patients with coronary artery disease, there were no correlations between any markers evaluated in this study (GHSR and ghrelin: $r = 0.3942$, $P = 0.1826$; GHSR and BNP: $r = 0.0596$, $P = 0.8467$; ghrelin and BNP: $r = 0.1769$, $P = 0.8850$; SERCA2a and GHSR: $r = 0.4132$, $P = 0.2354$; SERCA2a and ghrelin: $r = 0.5175$, $P = 0.1256$; SERCA2a and BNP: $r = 0.4315$, $P = 0.2131$). Sixteen patients had elevated estimated pulmonary artery pressures, on the basis of their preoperative echocardiograms and only 2 patients had a reduced ejection fraction before surgery (30%-40%). After cardiac surgery, 10 patients were receiving β-blockers, 11 were receiving diuretics, and 14 were receiving statins (Table 2).

### Correlations between GHSR and ghrelin in diseased cardiac tissue

Fluorescence intensities of GHSR and ghrelin were variable in any given cardiac tissue sample in the diseased and control
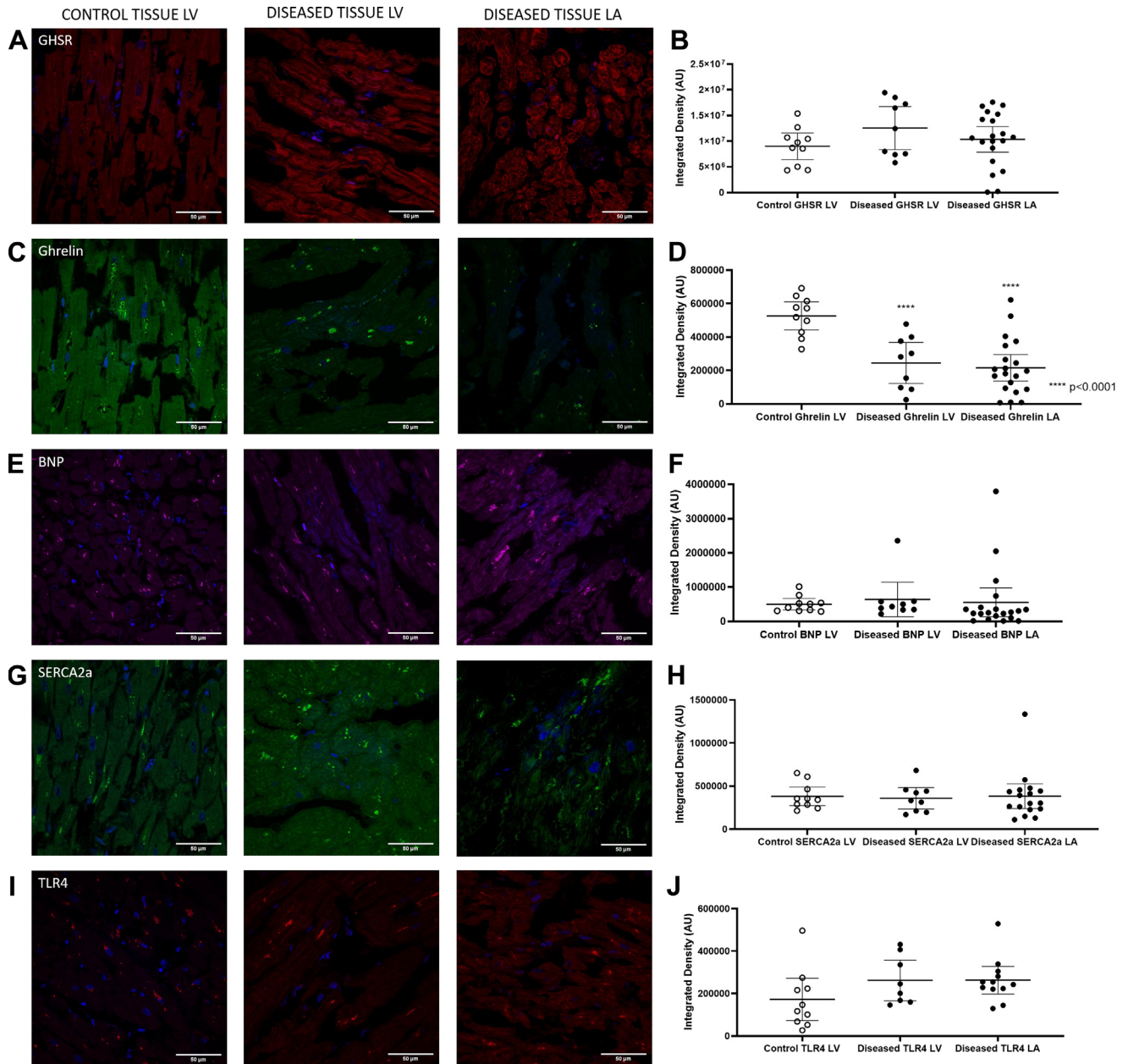
**Figure 1.** Representative confocal fluorescence images of all biomarkers (**A**) ([Dpr$^3$(n-octanoyl),Lys$^{19}$(sulfo-Cy5)]ghrelin(1-19): **red**; (**C**) ghrelin, **green**, (**E**) natriuretic peptide type-B (BNP), **magenta**; (**G**) sarcoplasmic reticulum ATPase pump (SERCA2a), **green**; (**I**) toll like receptor 4 [TLR4], **red**) in the control tissue left ventricle (LV; **left column**) and diseased tissue LV (**middle column**) and left atrium (LA; **right column**). All images indicate DAPI nuclear stain in **blue**. Graphs represent quantification of fluorescent images as mean ± 95% confidence interval of integrated densities for each biomarker with each dot representing one patient sample. There were no significant differences in fluorescence intensities of (**B**) Cy5-ghrelin(1-19) (control LV n = 10, LV n = 9, left atrium [LA] n = 20), (**F**) BNP (control LV n = 10, LV n = 9, LA = 20), (**H**) SERCA2a (control LV n=10, LV n = 9, LA = 17], or (**J**) TLR4 (control LV n = 10, LV n = 8, LA = 12]. There was a significant decrease in the fluorescence intensities detecting (**D**) ghrelin ($P < 0.0001$; control LV n = 10, LV n = 9, LA = 20] in the diseased cohort compared with the control tissues.

cohort (Fig. 1A and C). Overall GHSR expression was not significantly different between the diseased and control groups (Fig. 1B) whereas tissue ghrelin was significantly lower ($P < 0.0001$) in the diseased cohort in the left atrium and the left ventricle (Fig. 2D). Linear regression analysis of GHSR vs ghrelin showed a positive relationship in the overall cardiac surgery cohort ($r = 0.3995$; $P = 0.0318$; Fig. 2C). Regionally, this correlation persisted only in the left atrium ($r = 0.4859$;

$P = 0.0299$) and not in the left ventricle (Fig. 2D). There was no significant correlation between GHSR and ghrelin in the control tissues ($r = 0.1105$; $P = 0.3480$; Fig. 2B).

### Relationship of BNP to GHSR and ghrelin in diseased cardiac tissue

Fluorescence images indicated the localization of BNP within the diseased and control heart tissue (Fig. 1E). Analysis
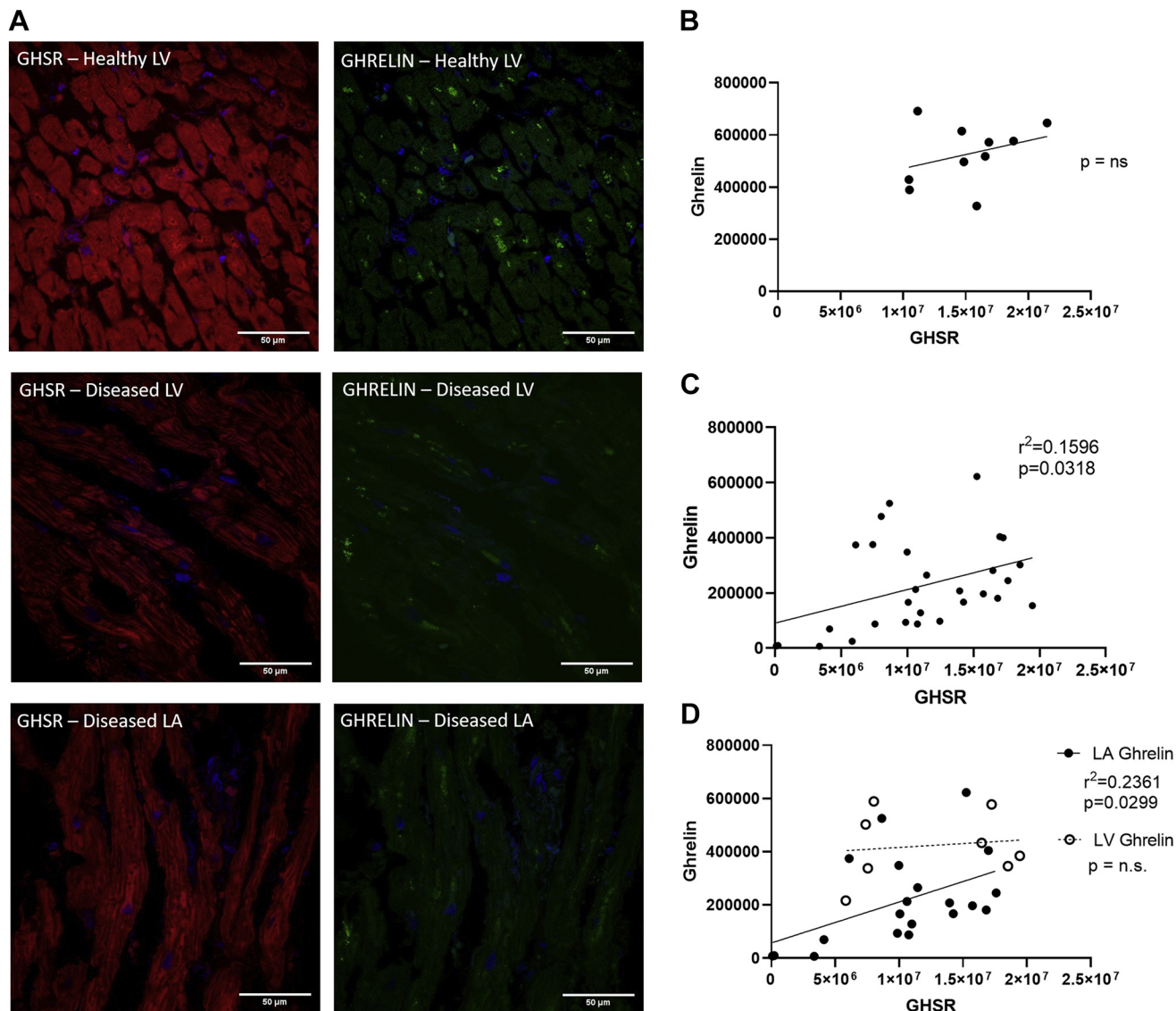
Sullivan et al.
Regional Ghrelin-GHSR Signalling in Heart Disease

187



**Figure 2.** Growth hormone secretagogue receptor (GHSR) and ghrelin fluorescence intensity in human cardiac tissue. (**A**) Representative confocal images of [Dpr$^3$(n-octanoyl),Lys$^{19}$(sulfo-Cy5)]ghrelin(1-19; Cy5-ghrelin(1-19); (**red**) and ghrelin (**green**) in diseased control left ventricle (LV; **top**), diseased LV (**middle**), and diseased left atrium (LA; **bottom**). DAPI (**blue**) indicates nuclear localization in cardiomyocytes. Graphs indicate quantification of integrated densities using linear regression between Cy5-ghrelin(1-19) and ghrelin. (**B**) In control tissue, there was no correlation between Cy5-ghrelin(1-19) and ghrelin (P = not significant [ns]; n = 10). (**C**) Linear regression between Cy5-ghrelin(1-19) and ghrelin (r = 0.3995; P = 0.0318) in the entire patient cohort (n = 29), where each dot represents 1 patient sample. (**D**) Regional analysis showed a significant linear regression of Cy5-ghrelin(1-19) and ghrelin in the LA (r = 0.4859; P = 0.0299; n = 20) but not the LV (P = ns; n = 9).

of these images indicated no significant difference in immunofluorescence (P = not significant) in the disease cohort compared with the control tissues (Fig. 1F). Linear regression analysis indicated a strong and significant positive relationship between BNP and GHSR (r = 0.5633; P = 0.0034); this relationship was strong within the left atrium (r = 0.6751; P = 0.0029) but not the left ventricle (r = 0.0127; P = 0.9784; Fig. 3C and D). There was also a significant positive relationship between BNP and ghrelin in the entire cohort (r = 0.5008; P = 0.0108). This relationship, however, differed according to region: left ventricle (r = 0.9152; P = 0.0014), left atrium (r = 0.394; P = 0.1177; Fig. 3E and F). Again, no relationship was seen between BNP and GHSR or

ghrelin in the control cardiac tissue (r = 0.2465; P = 0.4923 and r = 0.1236; P = 0.7337, respectively).

## Intracellular colocalization of ghrelin and BNP in cardiomyocytes

Ghrelin and BNP appeared to be spatially localized to the same intracellular compartment within cardiomyocytes. In the control tissue, ghrelin and BNP appeared as larger ordered punctate areas mainly surrounding the nucleus (Fig. 4A) whereas in the diseased tissue these colocalized areas of ghrelin and BNP were smaller and scattered more diffusely throughout the cell, and were not focused primarily around the nucleus (Fig. 4B and C). The Pearson
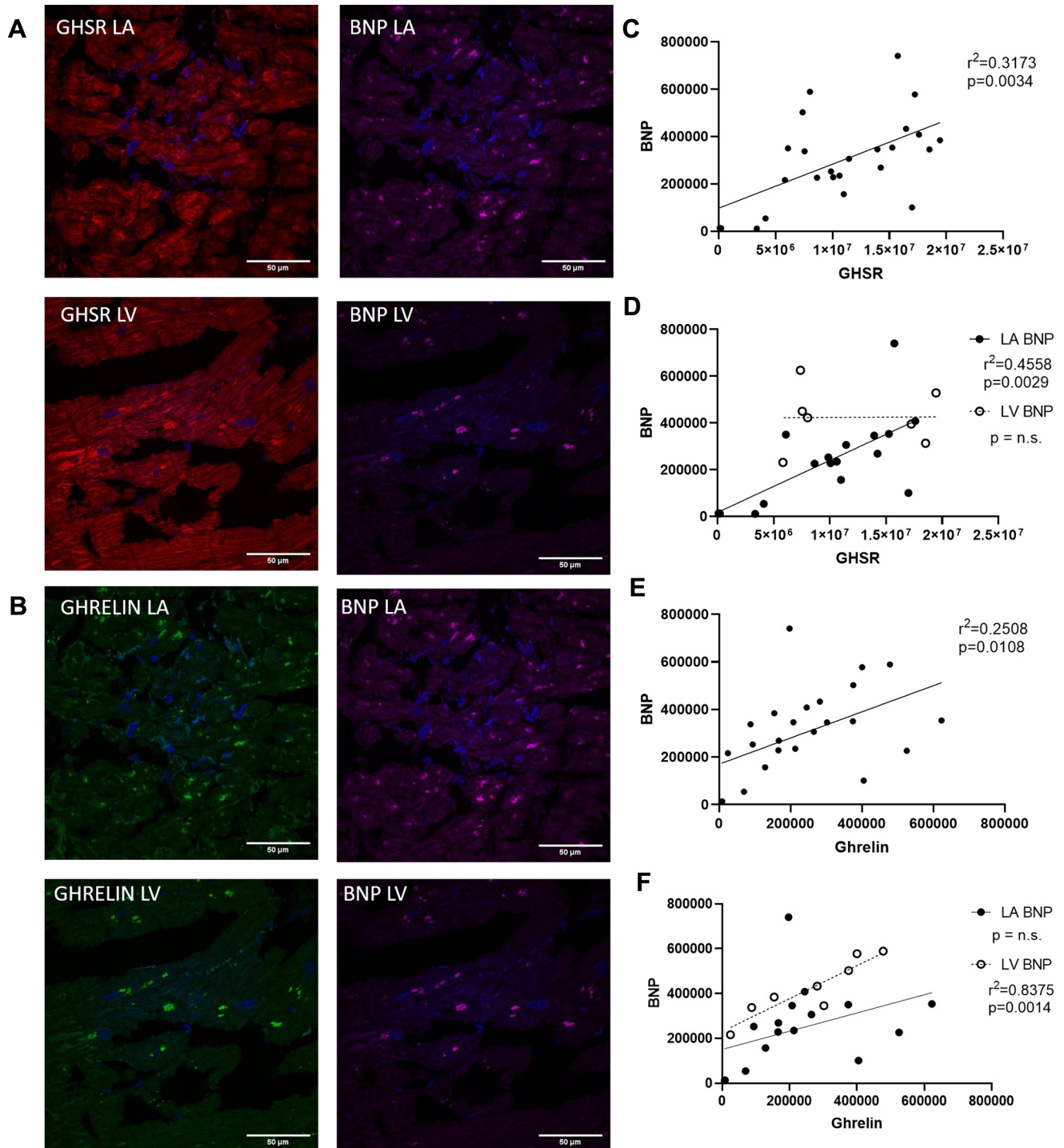
**Figure 3.** (**A** and **B**) Representative fluorescent confocal images of [Dpr$^3$(n-octanoyl),Lys$^{19}$(sulfo-Cy5)]ghrelin(1-19); **red**), ghrelin (**green**), and natriuretic peptide type-B (BNP; **magenta**) in human cardiac tissue in the left atrium (LA) and left ventricle (LV). Nuclei were visualized with DAPI (**blue**). Graphs show linear regression analysis of quantified integrated densities with each dot representing an individual patient sample. (**C**) There was significant linear regression of [Dpr$^3$(n-octanoyl),Lys$^{19}$(sulfo-Cy5)]ghrelin(1-19) vs BNP ($r$ = 0.5633; $P$ = 0.0034) in the entire patient cohort ($n$ = 25). (**D**) When data were disaggregated by region, a significant linear regression was found in the LA ($r$ = 0.6751; $P$ = 0.0029; n = 17) but not the LV ($P$ = not significant [ns]; n = 8). (**E**) Ghrelin and BNP were correlated in the entire patient cohort ($r$ = 0.5008; $P$ = 0.0108; n = 25). (**F**) Linear regression analysis between ghrelin and BNP indicate correlations in the LV ($r$ = 0.9152; $P$ = 0.0014; n = 17) but not the LA ($P$ = ns; n = 9). GHSR, growth hormone secretagogue receptor.

Sullivan et al.
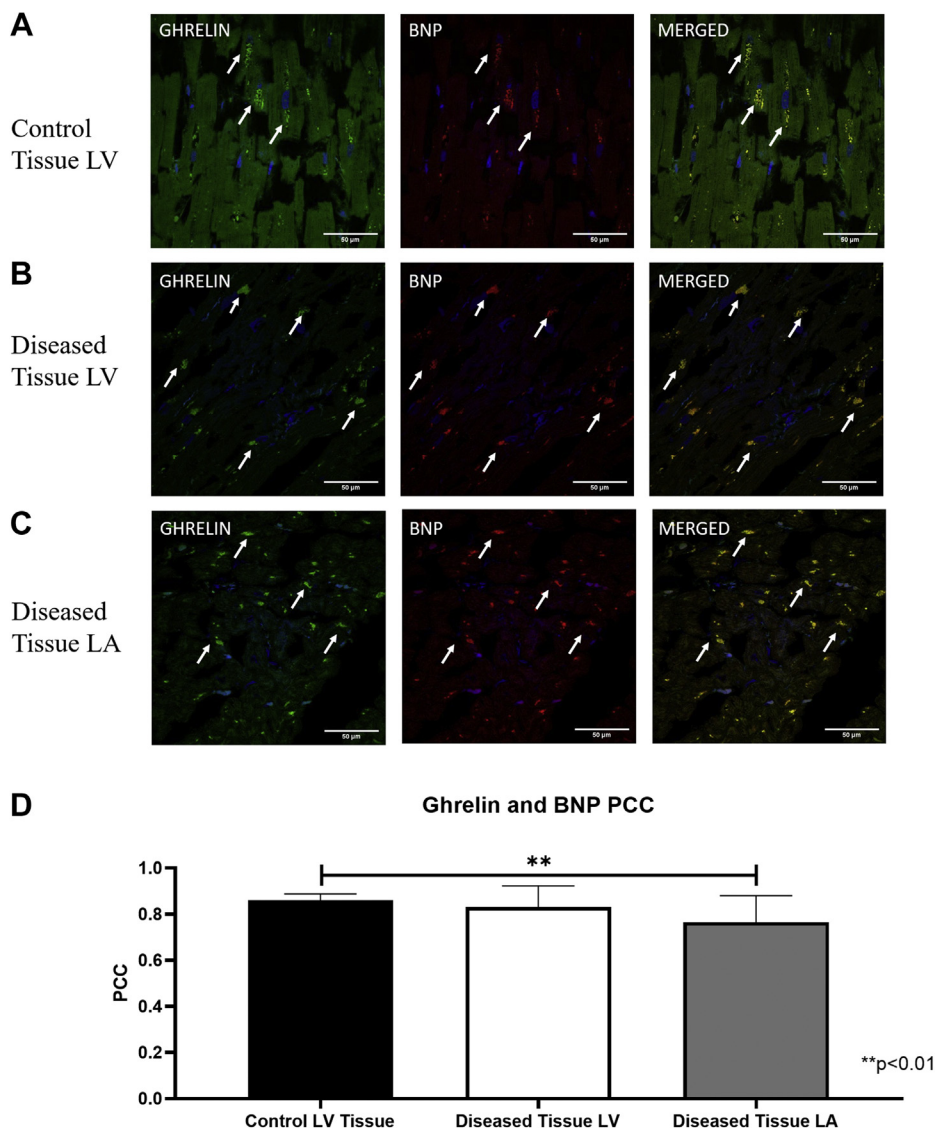Regional Ghrelin-GHSR Signalling in Heart Disease

189



**Figure 4.** Intracellular colocalization of ghrelin and natriuretic peptide type-B (BNP) in (**A**) control left ventricle (LV), (**B**) diseased LV tissue, and (**C**) left atrium (LA). (**A-C**) Representative confocal fluorescent images of ghrelin (**green**) and BNP (**red**) in healthy and diseased tissue shows correlation of ghrelin and BNP in the merged images. DAPI (**blue**) indicates nuclear staining. **White arrows** indicate areas of punctate staining and colocalization in the merged images. (**D**) Pearson coefficient correlation (PCC) values indicate a stronger correlation in the healthy tissue (n = 10) compared with the diseased tissue in the LA ($P = 0.0040$; n = 29) but not the LV ($P =$ not significant; n = 29). Values are mean $\pm$ SD.

correlation coefficient (PCC) was strong for diseased left atrium (PCC = 0.76), left ventricle (PCC = 0.83), and control (PCC = 0.86) whereas there was a significantly higher correlation in the control tissues compared with the LA ($P = 0.00169$) but not LV ($P = 0.2923$) diseased tissue (Fig. 4D).

**The relationship of the cardiac contractility biomarker SERCA2a to ghrelin and GHSR in the diseased heart**

Quantitative fluorescence microscopy was used to measure SERCA2a in the control and diseased cohorts with representative images shown in Fig. 1G. No differences in overall expression were seen between the diseased and control cohorts (Fig. 1H). Linear regression analysis showed that SERCA2a had a positive relationship to GHSR, ghrelin, and BNP (Fig. 5C-E) but only in the LV ($r = 0.7893$, $P = 0.0348$;

$r = 0.7315$, $P = 0.0392$; $r = 0.8401$, $P = 0.0180$, respectively) and not the LA. Quantification of overall expression of TLR4 showed no differences between the diseased and control cohorts (Fig. 1J). No relationships were present in the control group between SERCA2a and any other biomarker (GHSR: $r = 0.0936$, $P = 0.7970$; ghrelin: $r = 0.0089$, $P = 0.9385$; BNP: $r = 0.2492$, $P = 0.4875$).

**Cardiac fibrosis**

Masson's trichrome staining was used to determine the extent of fibrosis in all cardiac tissue samples. There were highly variable amounts of fibrotic deposition (blue) in samples of diseased tissue compared with the nonfibrotic tissue (red) in any given cardiac surgery patient sample but not in the control tissue (Fig. 6A-C). Quantification of the amount
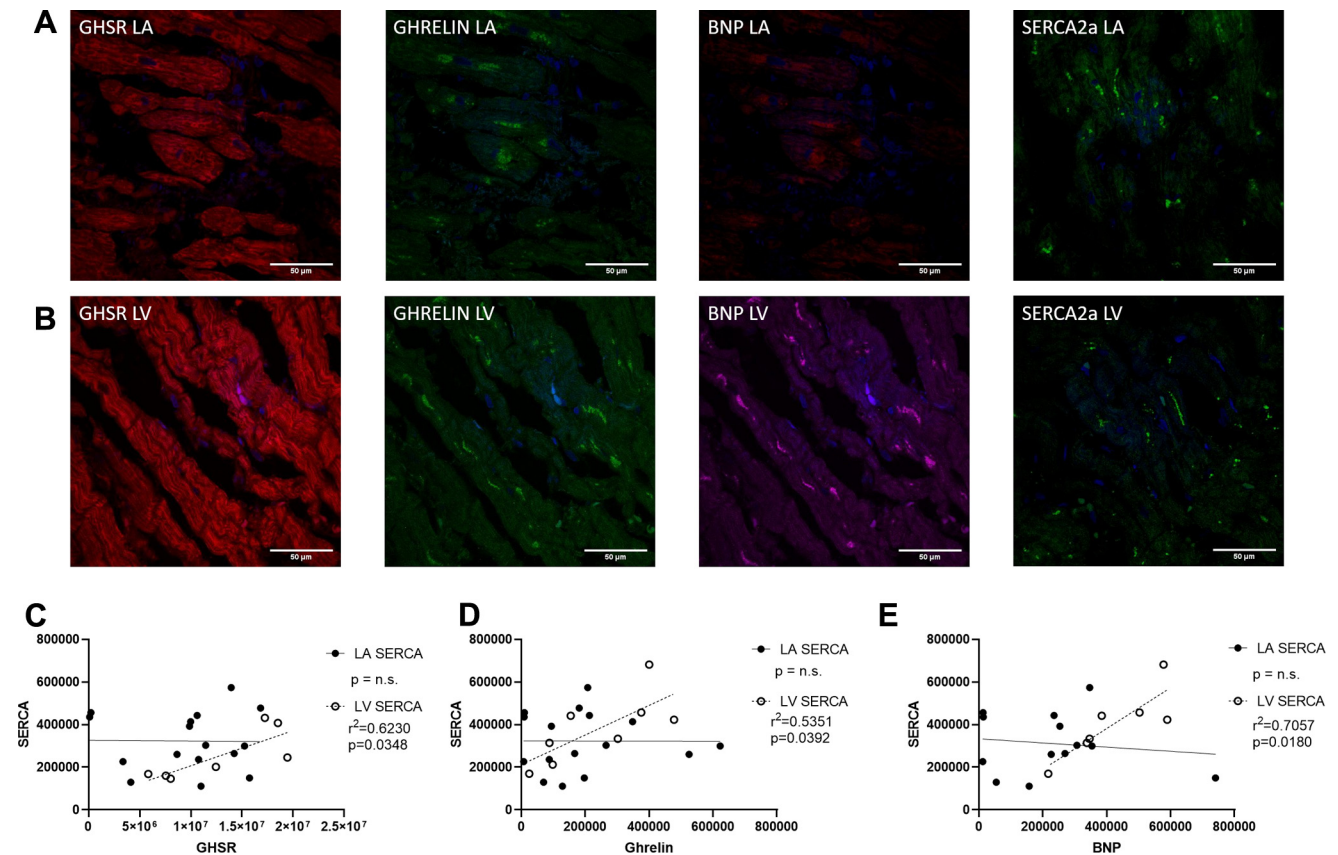
**Figure 5.** (**A**) Representative fluorescent confocal images of [Dpr³(n-octanoyl),Lys¹⁹(sulfo-Cy5)]ghrelin(1-19) (Cy5-ghrelin(1-19; **red**), ghrelin (**green**), natriuretic peptide type-B (BNP) (**magenta**), and sarcoplasmic reticulum ATPase pump (SERCA2a; **green**) in cardiac tissue of the left atrium (LA; **A** in top panels) and the left ventricle (LV; **B** middle panels). DAPI (**blue**) nuclear stain in all images. Graphs indicate fluorescence intensities represented by integrated densities where each dot represents 1 patient sample. A significant linear regression is present in only the LV between SERCA2a and (**C**) Cy5-ghrelin(1-19; $r = 0.7893$; $P = 0.0348$; LA n = 15, LV n = 8), (**D**) ghrelin ($r = 0.7315$; $P = 0.0392$; LA n = 15, LV n = 8), and (**E**) natriuretic peptide type-B (BNP; $r = 0.8401$; $P = 0.0180$; LA n = 14, LV n = 7).

of fibrotic tissue showed a significantly higher amount of collagen deposition in diseased tissues of the LA ($P = 0.0034$) but not of the LV ($P = 0.0509$) compared with the control tissues (Fig. 6D).

## Discussion

In this study, we used our fluorescent ghrelin analogue, Cy5-ghrelin(1-19), to examine the expression of myocardial GHSR in relation to that of ghrelin and other known markers of downstream signalling pathways in tissue obtained from patients with valvular heart/coronary artery disease but without reduced LVEF. We also measured these markers in control, nondiseased, cardiac tissue. In patients with valvular HD (with or without coronary artery disease), there were positive correlations between GHSR and ghrelin, which were regionally constrained to the left atrium. Similarly, there were regionally divergent correlations between GHSR and BNP (the gold standard marker of HF) and ghrelin and BNP. The positive correlations with the contractility marker SERCA2a were specific to the left ventricle. In contrast, no correlations between GHSR and ghrelin, or any other biochemical marker were observed in the control tissue. Additionally, we found

that ghrelin and BNP localized to the same intracellular compartment within cardiomyocytes, and this colocalization was slightly disrupted in the left atrium in the HD cohort. Therefore, there was an emergence of region-specific patterns in the myocardial ghrelin-GHSR signalling axis in patients with valvular disease despite the absence of measurable changes in heart function.

We have previously shown that GHSR and ghrelin are positively correlated in tissue samples from patients with end-stage HF and are correlated negatively with LVEF.[11] Results from other studies also indicate changes in the dynamics of the ghrelin-GHSR axis in end-stage HF[10] and dilated cardiomyopathy,[12] suggesting this cardioprotective ghrelin-GHSR system is abnormally upregulated when there is injury or stress to the heart.[11] Our present results also show a positive correlation between ghrelin and GHSR in patients with HD, but this time in the absence of a decrease in LVEF. Because this correlation was not observed in tissue samples from the control group, we suggest that changes in the myocardial ghrelin-GHSR axis occur early in the progression of HD (in this study, in hearts subject to increased LV systolic pressures secondary to aortic stenosis) before measurable changes in heart function, as defined by the global LV ejection fraction.
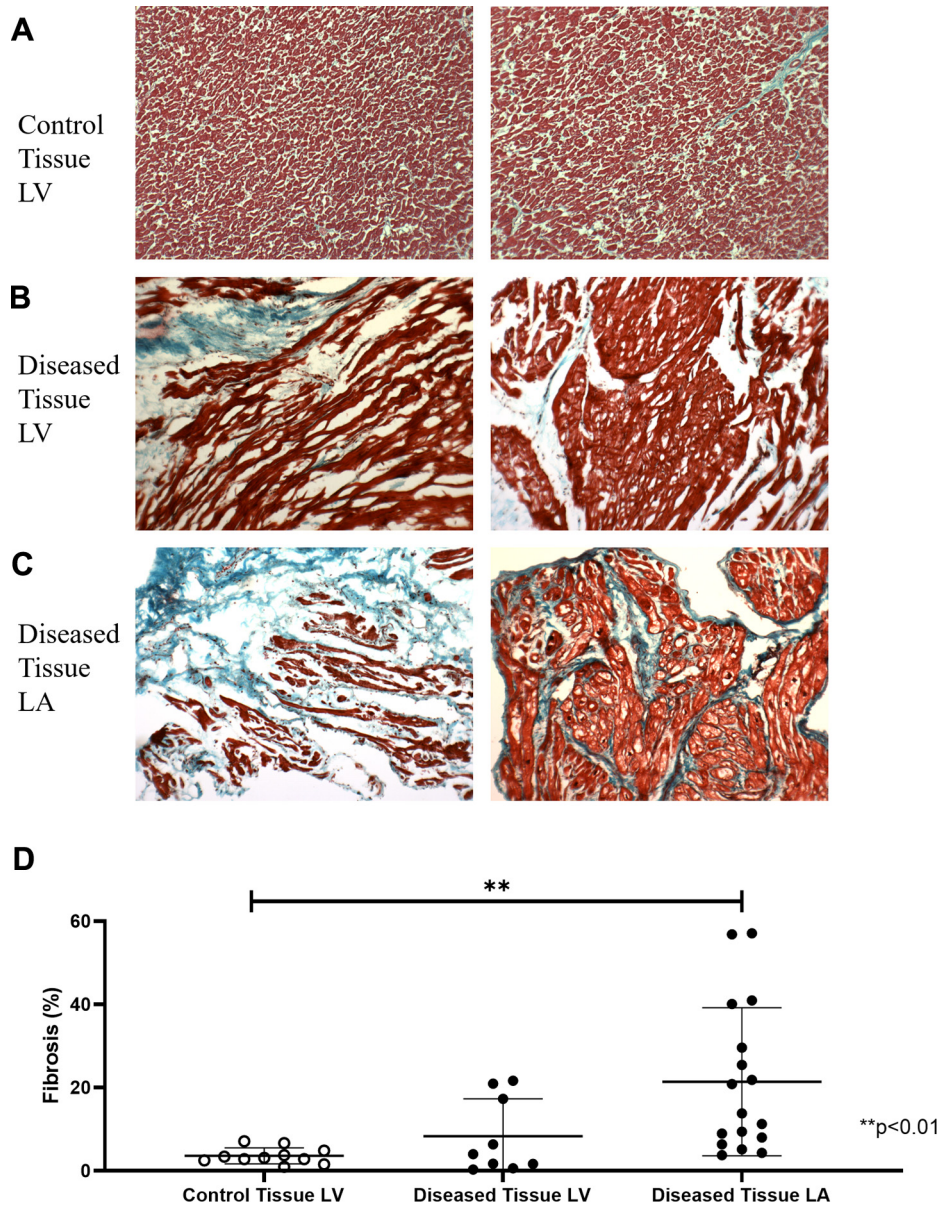
Sullivan et al.
Regional Ghrelin-GHSR Signalling in Heart Disease

191



**Figure 6.** Fibrosis deposition in healthy and diseased tissue. Representative images of fibrotic (**blue**) and nonfibrotic tissue (**red**) in (**A**) control left ventricle (LV) tissue and diseased tissues of the (**B**) LV and the (**C**) left atrium (LA) show variability in fibrotic deposition in the diseased tissue and not in the control tissue. (**D**) Graph shows mean ± 95% confidence interval of percentage fibrotic tissue with significantly less fibrotic deposition in the control tissue (n = 10) compared with the left atrium ($P$ = 0.0034; n = 17) but not the left ventricle ($P$ = not significant; n=11).

Post-hoc disaggregation of data according to region showed that the positive correlation between ghrelin and GHSR was maintained in the left atrium but not the left ventricle. Interpretation of these data is very limited because we did not collect data on the LA pressures that are commonly elevated in valvular diseases due to stretching of the atrial wall. We did, however, observe a very slight but significant negative correlation between GHSR in the left atrium and LV diastolic pressure ($r = 0.6887$; $P = 0.0402$). Left ventricular diastolic pressure is elevated in valve disease which is associated with increased LA pressure.[24] In one study by Schwarz et al., in patients with aortic valve disease, there was an elevation in end-diastolic LV pressure and mean LA pressure along with significant correlations with myocardial cell diameter.[25] Therefore, in our study of patients with aortic stenosis, it is expected that with the increased LV diastolic pressure, LA pressures are also increased. The increased LA pressures might be related to the strong correlation between ghrelin and GHSR. The positive GHSR-ghrelin correlation in the left atrium but not the left ventricle might also represent a compensatory upregulation under conditions of mild stress and trauma of the left atrium without any measurable changes in the heart function measured according to the LVEF. An upregulation might be increased through GHSR signalling in the left atrium, which promotes cardiomyocyte survival (through Akt and phosphorylated extracellular signal-regulated kinase)[5], contractility (through SERCA2a),[26] and inhibits signalling through proinflammatory proteins and apoptosis,[6,27] More robust data will be required to establish a concrete relationship

between alterations in the ghrelin-GHSR axis and onset of LA dysfunction.

In addition to the myocardium, ghrelin and GHSR are also present in the endothelial cells of the aorta, coronary arteries, and pulmonary arteries and veins.[28] Ghrelin is known to have vasoconstrictive effects in the coronary arteries and dose-dependently increases coronary perfusion pressure in a calcium-dependent manner, thereby enhancing arteriole contractility.[29] The density of GHSR is increased in the atherosclerotic coronary artery and the saphenous vein compared with the corresponding nondiseased artery and vein,[30] indicating that upregulation of ghrelin-GHSR signalling might occur within the diseased vasculature. In the same study, no differences in GHSR density were observed in the left atrium or the left ventricle between the ischemic HD or dilated cardiomyopathy to the control tissues.[30] Our findings also showed no changes in myocardial GHSR as measured by Cy5-ghrelin(1-19), and a relatively weak correlation with ghrelin, suggesting that more dramatic changes in GHSR might occur at the site of vascular tissue injury or dysfunction.

The secretion of BNP and its N-terminal form, the current "gold standard" clinical HF biomarkers, are increased under conditions of cardiomyocyte stress and pressure overload. Circulating BNP levels are also increased in patients with aortic stenosis and mitral regurgitation, and can be used as a potential indication for valve replacement in patients with normal ejection fraction.[31] However, myocardial BNP mRNA does not change in patients who had aortic valve stenosis.[32] In our current study in patients with valvular disease, we also did not find a change in the tissue expression of BNP in either the left atrium or the left ventricle. If tissue levels of BNP do not change, but levels of circulating BNP increase in valvular disease, it might suggest that the rate of post-translational processing of pro-BNP, rather than transcription or translation, increases in cardiomyocytes.

Interestingly, we found that BNP and ghrelin correlated in the left ventricle, and furthermore, strongly colocalized to the same intracellular compartment within ventricular cardiomyocytes. In healthy individuals, BNP is predominantly localized in the atrium; in patients with HF, BNP appears to localize primarily in the ventricles.[33] In patients with aortic stenosis, the endocrine profile of aortic valves, which includes natriuretic peptides, their receptors, and processing enzymes, is altered[32]; taken together with our results, we suggest that a regional shift in myocardial endocrine programming might be part of the progression of HD to HF. This regional shift might extend to other genetic programs as well; in dogs exposed to prolonged rapid ventricular pacing, there were drastic changes in genes expressing apoptosis, cell structure and mobility, and inflammation in the left atrium, whereas genes involved in metabolism and $Ca^{2+}$ signalling changed only in the left ventricle.[34,35] Therefore, there are clear regional differences in the genetic programs that underlie cardiomyocyte function in HD. Further studies will determine the intracellular dynamics of ghrelin and BNP during the progression of HD.

We also evaluated GHSR signalling pathways involving contractility and inflammation. We were particularly interested in correlations with SERCA2a, a common marker of contractility, as it has been shown to be activated through the GHSR signalling pathway, reducing intracellular $Ca^{2+}$ levels,

and improving LVEF after myocardial infarction.[2] Additionally, we have previously found strong relationships between ghrelin and SERCA2a in a mouse model of cardiomyopathy[13] and human HF.[11] In the present study, we observed a positive correlation between SERCA2a and ghrelin-GHSR only in the left ventricle, which might indicate the importance of contractility signalling in the left ventricle, because it is the predominant chamber for contractile force. Activation of GHSR is known to regulate calcium handling and cardiomyocyte relaxation. This positive correlation in the left ventricle might indicate the promotion of contractile function in the heart through GHSR by enhancing SERCA2a function. GHSR activation causes $G\alpha q11$ to activate the protein kinase A/calmodulin-dependent phosphokinases pathway through phosphorylation of phospholamban from SERCA2a on the sarcoplasmic reticulum membrane, thereby eliminating the inhibitory effect of phospholamban on SERCA2a uptake.[26] Removal of this inhibition increases the calcium flux in the sarcoplasmic reticulum thereby decreasing intracellular calcium and promoting contractility.[2,26] Additionally, SERCA2a and BNP were also correlated only in the left ventricle. Through binding natriuretic peptide receptor-A, BNP activates cyclic guanosine monophosphate signalling, which is coupled to L-type calcium channels and intracellular calcium levels through SERCA2a in ventricular cardiomyocytes.[36] Because LVEF was unchanged in most of the patients, it is likely that alterations in the relationships between SERCA2a, ghrelin-GHSR, and BNP within LV cardiomyocytes occurs before any overt functional changes detected using echocardiography.

TLR4 is a marker of inflammation elevated in the myocardium in end stage HF,[37,38] and ghrelin has been shown to attenuate the proinflammatory effects of TLR4 in patients with HF.[4,39] In this study, we did not find any significant correlations between TLR4 and GHSR or ghrelin or other biomarkers, which might indicate the TLR4-mediated proinflammatory axis is not coregulated with the ghrelin-GHSR system at this point in valvular HD.

Another measure of cardiac damage is the presence of fibrosis (collagen and fibroblast deposition) in the myocardium, which increases with HD severity.[40,41] Our results indicate a significant increase in the fibrotic deposition in only the left atrium of patients with HD compared with the control heart tissues. The apparent lack of LV fibrosis is consistent with the preserved LVEF of this cohort.[42] This accumulation of fibrosis present in the left atrium might be associated with the downstream signalling pathway changes seen in ghrelin-GHSR in this cohort because increased fibrosis deposition is common in the heart during the later stages of HF and is a sign of cardiomyocyte damage. However, these results are a bit difficult to interpret because of the large degree of variability in fibrosis in the patient cohort. This result is not surprising because of the heterogenous nature of fibrosis deposition in the myocardium and the subsequent difficulty in obtaining representative biopsy specimens.[43]

There are a few limitations to our study to note. Our study was conducted with a small sample size that limited effective disaggregation of the data according to region. It is important to note that the control and diseased tissues were embedded differently (paraffin wax vs fixed frozen respectively), although all samples were stained with the same protocols for each

Sullivan et al.
Regional Ghrelin-GHSR Signalling in Heart Disease

193

marker tested. Quantification of paraffin and frozen healthy heart tissue is shown in Supplemental Figure S2, in which it is shown that there was no difference in the quantification between either tissue storage method. In addition, control LV tissue was obtained up to 1-3 days postmortem which could allow for potential protein degradation between time of death and when the tissue samples were put in fixative during autopsy. Finally, we did not obtain blood samples from the patients, which would have provided useful insight into the relationship between myocardial and circulating levels of ghrelin and BNP.

To conclude, we have identified changes in the myocardial ghrelin-GHSR axis in human valvular HD compared with control cardiac tissues. The correlation between ghrelin and BNP and the colocalization in the myocardium of these peptides might suggest a regional shift in myocardial endocrine programming of cardiac cells in valvular HD. We have shown that the contractility marker SERCA2a was selectively correlated in the left ventricle, potentially as a cardioprotective mechanism before decreased LVEF. Our ongoing work will help to characterize GHSR-associated biochemical changes present in early stages of HD.

## Disclosures

The authors have no conflicts of interest to disclose.

## References

1. Ma Y, Zhang L, Launikonis BS, Chen C. Growth hormone secretagogues preserve the electrophysiological properties of mouse cardiomyocytes isolated from in vitro ischemia/reperfusion heart. Endocrinology 2012;153:5480-90.

2. Ma Y, Zhang L, Edwards JN, Launikonis BS, Chen C. Growth hormone secretagogues protect mouse cardiomyocytes from in vitro ischemia/reperfusion injury through regulation of intracellular calcium. PLoS One 2012;7:e35265.

3. Raghay K, Akki R, Bensaid D, Errami M. Ghrelin as an anti-inflammatory and protective agent in ischemia/reperfusion injury. Peptides 2019;124:170226.

4. Wang Q, Lin P, Li P, et al. Ghrelin protects the heart against ischemia/reperfusion injury via inhibition of TLR4/NLRP3 inflammasome pathway. Life Sci 2017;186:50-8.

5. Baldanzi G, Filigheddu N, Cutrupi S, et al. Ghrelin and des-acyl ghrelin inhibit cell death in cardiomyocytes and endothelial cells through ERK1/2 and PI 3-kinase/AKT. J Cell Biol 2002;159:1029-37.

6. Huang CX, Yuan MJ, Huang H, et al. Ghrelin inhibits post-infarct myocardial remodeling and improves cardiac function through anti-inflammation effect. Peptides 2009;30:2286-91.

7. Yang C, Liu Z, Liu K, Yang P. Mechanisms of ghrelin anti-heart failure: Inhibition of ang II-induced cardiomyocyte apoptosis by down-regulating AT1R expression. PLoS One 2014;9:e85785.

8. Wang Q, Sui X, Chen R, et al. Ghrelin ameliorates angiotensin II-induced myocardial fibrosis by upregulating peroxisome proliferator-activated receptor gamma in young male rats. Biomed Res Int 2018;2018:9897581.

9. Yang C, Liu J, Liu K, et al. Ghrelin suppresses cardiac fibrosis of post-myocardial infarction heart failure rats by adjusting the activin A-follistatin imbalance. Peptides 2018;99:27-35.

10. Beiras-Fernandez A, Kreth S, Weis F, et al. Altered myocardial expression of ghrelin and its receptor (GHSR-1a) in patients with severe heart failure. Peptides 2010;31:2222-8.

11. Sullivan R, Randhawa VK, Stokes A, et al. Dynamics of the ghrelin/growth hormone secretagogue receptor system in the human heart before and after cardiac transplantation. J Endocr Soc 2019;3:748-62.

12. Aleksova A, Beltrami AP, Bevilacqua E, et al. Ghrelin derangements in idiopathic dilated cardiomyopathy: impact of myocardial disease duration and left ventricular ejection fraction. J Clin Med 2019;8:1152-72.

13. Sullivan R, McGirr R, Hu S, et al. Changes in the cardiac GHSR1a-ghrelin system correlate with myocardial dysfunction in diabetic cardiomyopathy in mice. J Endocr Soc 2018;2:178-89.

14. Pei XM, Yung BY, Yip SP, et al. Protective effects of desacyl ghrelin on diabetic cardiomyopathy. Acta Diabetol 2015;52:293-306.

15. Fox KF, Cowie MR, Wood DA, et al. Coronary artery disease as the cause of incident heart failure in the population. Eur Heart J 2001;22:228-36.

16. Kadoglou NP, Lampropoulos S, Kapelouzou A, et al. Serum levels of apelin and ghrelin in patients with acute coronary syndromes and established coronary artery disease-KOZANI STUDY. Transl Res 2010;155:238-46.

17. Zhang M, Fang WY, Yuan F, et al. Plasma ghrelin levels are closely associated with severity and morphology of angiographically-detected coronary atherosclerosis in Chineses patients with diabetes mellitus. Acta Pharmacol Sin 2012;33:452-8.

18. Wang F, Jiang T, Tang C, et al. Ghrelin reduces rat myocardial calcification induced by nicotine and vitamin D3 in vivo. Int J Mol Med 2011;28:513-9.

19. Li GZ, Jiang W, Zhao J, P, et al. Ghrelin blunted vascular calcification in vivo and in vitro in rats. Regul Pept 2005;129:167-76.

20. McGirr R, McFarland MS, McTavish J, Luyt LG, Dhanvantari S. Design and characterization of a fluorescent ghrelin analog for imaging the growth hormone secretagogue receptor 1a. Regul Pept 2011;172:69-76.

21. Douglas GA, McGirr R, Charlton CL, et al. Characterization of a far-red analog of ghrelin for imaging GHS-R in P19-derived cardiomyocytes. Regul Pept 2014;54:81-8.

22. Locatelli V, Rossoni G, Schweiger F, et al. Growth hormone-independent cardioprotective effects of hexarelin in the rat. Endocrinology 1999;140:4024-31.

23. Kennedy DJ, Vetteth S, Periyasamy SM, et al. Central role for the cardiotonic steroid marinobufagenin in the pathogenesis of experimental uremic cardiomyopathy. Hypertension 2006;47:488-95.

24. Braunwald E, Moscovitz HL, Amram SS, et al. The hemodynamics of the left side of the heart as studied by simultaneous left atrial, left ventricular, and aortic pressures; particular reference to mitral stenosis. Circulation 1955;12:69-81.

25. Schwarz F, Flameng W, Schaper J, Hehrlein F. Correlation between myocardial structure and diastolic properties of the heart in chronic aortic valve disease: effects of corrective surgery. Am J Cardiol 1978;42:895-903.

26. Warbrick I, Rabkin SW. Effect of the peptides relaxin, neuregulin, ghrelin and glucagon-like peptide-1, on cardiomyocyte factors involved in the molecular mechanisms leading to diastolic dysfunction and/or heart failure with preserved ejection fraction. Peptides 2019;111:33-41.

27. Yuan MMJ, Huang H, Huang CXC. Potential new role of the GHSR-1a-mediated signaling pathway in cardiac remodeling after myocardial infarction. Oncol Lett 2014;8:969-71.

28. Papotti M, Ghè C, Cassoni P, et al. Growth hormone secretagogue binding sites in peripheral human tissues. J Clin Endocrinol Metab 2000;85:3803-7.

29. Pemberton CJ, Tokola H, Bagi Z, et al. Ghrelin induces vasoconstriction in the rat coronary vasculature without altering cardiac peptide secretion. Am J Physiol Heart Circ Physiol 2004;287:1522-9.

30. Katugampola SD, Pallikaros Z, Davenport AP. [125I-His9]-Ghrelin, a novel radioligand for localizing GHS orphan receptors in human and rat tissue; up-regulation of receptors with atherosclerosis. Br J Pharmacol 2001;134:143-9.

31. Bergler-Klein J, Gyöngyösi M, Maurer G. The role of biomarkers in valvular heart disease: focus on natriuretic peptides. Can J Cardiol 2014;30:1027-34.

32. Peltonen TO, Taskinen P, Soini Y, et al. Distinct downregulation of C-type natriuretic peptide system in human aortic valve stenosis. Circulation 2007;116:1283-9.

33. Hystad ME, Geiran OR, Attramadal H, et al. Regional cardiac expression and concentration of natriuretic peptides in patients with severe chronic heart failure. Acta Physiol Scand 2001;171:395-403.

34. Cardin S, Pelletier P, Libby E, et al. Marked differences between atrial and ventricular gene-expression remodeling in dogs with experimental heart failure. J Mol Cell Cardiol 2008;45:821-31.

35. Pelouch V, Milerová M, Ošťádal B, Hučín B, Šamánek M. Differences between atrial and ventricular protein profiling in children with congenital heart disease. Mol Cell Biochem 1995;147:43-9.

36. Rose RA, Giles WR. Natriuretic peptide C receptor signalling in the heart and vasculature. J Physiol 2008;586:353-66.

37. Yu L, Feng Z. The role of toll-like receptor signaling in the progression of heart failure. Mediators Inflamm 2018;2018:9874109.

38. Yang Y, Lv J, Jiang S, et al. The emerging role of toll-like receptor 4 in myocardial inflammation. Cell Death Dis 2016;26:e2234.

39. Liu SP, Li XY, Li Z, et al. Octanoylated ghrelin inhibits the activation of the palmitic acid-induced TLR4/NF-κB signaling pathway in THP-1 macrophages. ISRN Endocrinol 2012;2012:237613.

40. Barasch E, Gottdiener JS, Aurigemma G, et al. The association between elevated fibrosis markers and heart failure in the elderly: the Cardiovascular Health study. Circ Heart Fail 2009;2:303-10.

41. Travers J, Kamal F, Robbins J, Yutzey K, Blaxall B. Cardiac fibrosis. Circ Res 2016;118:1021-40.

42. Burlew BS, Weber KT. Cardiac fibrosis as a cause of diastolic dysfunction. PLoS One 2002;27:92-8.

43. Nagaraju CK, et al. Myofibroblast phenotype and reversibility of fibrosis in patients with end-stage heart failure. J Am Coll Cardiol 2019;73:2267-82.

## Supplementary Material

To access the supplementary material accompanying this article, visit *CJC Open* at https://www.cjcopen.ca/ and at https://doi.org/10.1016/j.cjco.2020.10.015.